



1974 ANNUAL REPORT
Under NASA Grant NGR 39-009-077

ON
INVESTIGATION OF CRITICAL BURNING
OF FUEL DROPLETS

by

G. M. Faeth and S. Chanin

Mechanical Engineering Department
The Pennsylvania State University
University Park, Pennsylvania



prepared for

NATIONAL AERONAUTICS AND SPACE ADMINISTRATION

NASA Lewis Research Center
Contract NGR 39-009-077

Richard J. Priem, Program Manager and Technical Monitor

(NASA-CR-134793) INVESTIGATION OF CRITICAL
BURNING OF FUEL DROPLETS Annual Report,
1974 (Pennsylvania State Univ.) 43 p. HC
\$3.-75 CSCI 21B Unclas
G3/25 14680

NOTICE

This work was prepared as an account of Government sponsored work. Neither the United States, nor the National Aeronautics and Space Administration (NASA), nor any person acting on behalf of NASA:

- A.) Makes any warranty or representation, expressed or implied, with respect to the accuracy, completeness, or usefulness of the information contained in this report, or that the use of any information, apparatus, method, or process disclosed in this report may not infringe privately owned rights; or
- B.) Assumes any liabilities with respect to the use of, or for damages resulting from the use of any information, apparatus, method or process disclosed in this report.

As used above, "person acting on behalf of NASA" includes any employee or contractor of NASA, or employee of such contractor, to the extent that such employee or contractor of NASA, or employee of such contractor prepares, disseminates, or provides access to, any information pursuant to his employment or contract with NASA, or his employment with such contractor.

1. Report No. NASA CR - 134793		2. Government Accession No.		3. Recipient's Catalog No.	
4. Title and Subtitle 1974 Annual Report on Investigation of Critical Burning of Fuel Droplets				5. Report Date February, 1975	
				6. Performing Organization Code	
7. Author(s) G. M. Faeth and S. Chanin				8. Performing Organization Report No.	
9. Performing Organization Name and Address Mechanical Engineering Department The Pennsylvania State University University Park, Pennsylvania 16802				10. Work Unit No.	
				11. Contract or Grant No. NGR 39-009-077	
12. Sponsoring Agency Name and Address National Aeronautics and Space Administration Washington, D.C. 20546				13. Type of Report and Period Covered Annual Report for 1974	
				14. Sponsoring Agency Code	
15. Supplementary Notes Project Manager, Richard J. Priem, Chemical Propulsion Division NASA Lewis Research Center, Cleveland, Ohio					
16. Abstract <p>The steady combustion characteristics of droplets has been considered in combustion chamber environments at various pressures, flow conditions and ambient oxidizer concentrations for a number of hydrocarbon fuels. Using data obtained earlier, predicted gasification rates were within $\pm 30\%$ of measurements when the correction for convection was based upon average properties between the liquid surface and the flame around the droplet. Analysis was also completed for the open loop response of monopropellant droplets, based upon earlier strand combustion results. At the limit of large droplets, where the effect of flame curvature is small, the results suggest sufficient response to provide a viable mechanism for combustion instability in the frequency and droplet size range appropriate to practical combustors. Calculations are still in progress for a broader range of droplet sizes, including conditions where active combustion effects are small.</p>					
17. Key Words (Suggested by Author(s)) Liquid Fuel Combustion High Pressure Combustion Hydrazine Fuel Combustion Burning Rate Response			18. Distribution Statement Unclassified - Unlimited		
19. Security Classif. (of this report) Unclassified		20. Security Classif. (of this page) Unclassified		21. No. of Pages 41	22. Price* \$3.00

* For sale by the National Technical Information Service, Springfield, Virginia 22151

1974 Annual Report on the Investigation
of Critical Burning of Fuel Droplets

Summary

This report discusses activities under NASA Contract NGR 39-009-077 for the period January 1, 1974 to December 31, 1974. During this period the work was divided into two phases: 1. High pressure droplet burning in flowing combustion gases and 2. Combustion response of monopropellant droplets. The results for each phase of the study for the present report period may be summarized as follows:

1. High Pressure Droplet Burning in Flowing Combustion Gases. Theory and experiment were compared over the currently available range of test data for droplet combustion in combustion gas environments. Predictions were within $\pm 30\%$ of measurements for a wide range of conditions when the model employed a multiplicative correction for convection based on average properties between the liquid surface and the flame. The range of comparison for these results is summarized in Table 1. With regard to liquid surface conditions, the low pressure model is adequate at pressures less than one half the pressure required for critical combustion, while the high pressure version provides a superior prediction at higher pressures. The two models do not overlap, however, within their range of validity. Therefore an intermediate pressure model, which is being developed to provide greater accuracy in this region, is presented in this report.
2. Combustion response of monopropellant droplets. Earlier response results for burning liquid monopropellant strands were applied directly to the discussion of the response of large droplets. The limits for the "large droplet" conditions are discussed. The results show sufficient response to provide a viable mechanism for combustion instability; in the frequency range associated with combustion instability and for droplet sizes present in sprays. The results also suggest that gas phase transient phenomena might contribute sufficient gain for combustion instability at low pressures. Thus although the gas phase might be considered quasisteady for lifetime calculations, important contributions to the response could be overlooked by this approach. The strand analysis has been converted to consider the combustion response of droplets under the same property assumptions. This model allows evaluation of the limits of the "large droplet" model to be determined as well as combustion response down to the limit of low reactivity (evaporative limit). Zero-order closed form solutions have been obtained for the evaporative limit. Numerical calculations are being conducted for the response and zero-order results for finite reactivity. A quasisteady gas phase model has also been completed.

Table of Contents

	<u>Page</u>
Summary	i
List of Figures	v
List of Tables	vi
I. Introduction	1
II. High Pressure Droplet Burning in Flowing Combustion Gases	3
2.1 Introduction	3
2.2 Experimental Data Correlation	3
2.3 Intermediate Pressure Model	9
2.4 Summary	12
III. Combustion Response of Monopropellant Droplets	13
3.1 Introduction	13
3.2 Large Droplet Limit	14
3.3 Droplet Response Analysis	19
3.3.1 Description and Assumptions of the Model	19
3.3.2 Governing Equations	24
3.3.3 Schvab-Zeldovich Transformation	27
3.3.4 Perturbation Analysis	28
3.4 Quasisteady Gas Phase Analysis	30
3.4.1 General Analysis	30
3.4.2 Gas Phase Analysis for Small A	32
3.4.3 Perturbation Analysis	33
3.5 Summary	34
References	35

List of Figures

	<u>Page</u>
1. Evaporation rate of methanol as a function of ambient temperature at atmospheric pressure. Approach Reynolds number range 46-174. Approach convection correction-darkened symbols; averaged convection correction-open symbols.	6
2. Gasification rates of n-heptane as a function of pressure for various ambient oxygen concentrations. Approach Reynolds number range 66-672. Approach convection correction-darkened symbols; averaged convection correction-open symbols.	7
3. Overall comparison of theoretical and experimental gasification rates in combustion gas environments. Lines A-A are data bounds when average properties are used in the convection correction.	8
4. Liquid surface temperatures as a function of pressure for the droplet combustion experiments of Ref. 8.	10
5. Liquid surface temperatures as a function of pressure for the strand combustion experiments of Ref. 9.	11
6. Computed Real Part of the Acoustic Admittance as a Function of Frequency and Pressure for Hydrazine.	15
7. Sketch of the droplet combustion response model.	20

List of Tables

	<u>Page</u>
1. Summary of Droplet Combustion Test Conditions	5
2. Critical Frequency Ranges for Hydrazine Strand Combustion	16
3. Hydrazine Droplet Sizes as a Function of Flame Position and Pressure.	18
4. Notation for Open Loop Response Analysis	21

1974 Annual Report on the Investigation
of Critical Burning of Fuel Droplets

1. Introduction

The objective of this study was to continue earlier work on the steady and unsteady combustion of liquid fuel droplets under rocket engine conditions. Emphasis has been placed on consideration of combustion at elevated pressures and temperatures representative of typical combustion chamber environments. In addition, the problem of the open-loop response of burning fuel droplets to imposed pressure oscillations is being investigated. The results of this study has technical application to the design of liquid fueled rocket engines and the determination of the combustion instability characteristics of these engines.

This report gives a summary of progress on the investigation for the period January 1, 1974 to December 31, 1974. During this period, the work was divided into two major phases, as follows:

1. High pressure droplet burning in flowing combustion gases. Earlier work provided data on droplet gasification rates in flowing combustion gases over a wide range of temperatures, pressures, ambient oxygen concentrations, fuels, and Reynolds numbers (1,2). This data was analyzed in an attempt to improve the prediction of gasification rates from the results of Ref. 1. Improvements have been made by modifying the correlation for convection effects. A second phase of this portion of the study involved developing an intermediate pressure, phase equilibrium model in order to obtain a continuous transition between the present low and high pressure versions.
2. Combustion response of monopropellant droplets. This portion of the study is concerned with extending the analysis of the "open loop" response of burning monopropellant strands (3), to the case of droplets. The basic method employs a perturbation analysis allowing for both liquid and gas phase transient effects. In addition, several simplified procedures are being considered. At high rates of reactivity (large droplets at high pressures), the combustion zone is located close to the droplet and the results of Ref. 3 can be used directly to discuss droplet response. At the other extreme, the analysis is considerably simplified when reaction rates are small and the droplet is simply evaporating. Finally, when the gas phase is quasisteady, consideration of response can be approached by using generalized transport relations which are also suitable for conducting droplet lifetime predictions.

The activities in each of these phases of the investigation will be discussed in the following sections of the report.

During this report period, several papers, theses and reports have been issued as a result of work done under this contract, as follows:

C. B. Allison, "Burning Rate Response of Liquid Monopropellants to Imposed Pressure Oscillations," NASA CR-134541, January 1974; also Ph.D. thesis, The Pennsylvania State University, University Park, PA, March 1974.

G. S. Canada, "High Pressure Combustion of Liquid Fuels," NASA CR-134540, January 1974, also Ph.D. Thesis, The Pennsylvania State University, University Park, PA, March 1974.

G. S. Canada and G. M. Faeth, "Combustion of Liquid Fuels in a Flowing Combustion Gas Environment," Fifteenth Symposium (International) on Combustion, Tokyo, August 1974, also The Combustion Institute, Pittsburgh, PA, (in press).

C. B. Allison and G. M. Faeth, "Open-Loop Response of a Burning Liquid Monopropellant," accepted for publication in AIAA J.

2. High Pressure Droplet Burning in Flowing Combustion Gases.

2.1 Introduction

The objectives of this phase of the investigation involve the determination of droplet vaporization rates and the characteristics (temperature, composition, etc.) of the liquid surface under forced convection conditions, at elevated pressures, in combustion chamber environments.

Work during the present report period involved continued comparison of earlier theoretical results with measurements of droplet gasification in combustion gases at elevated pressures. Work was also begun on the development of an intermediate pressure model to allow more accurate prediction of the phase equilibrium at the surface of a burning droplet than is currently possible.

2.2 Experimental Data Correlation

Work reported in Ref. 1 involved comparison between theoretical and experimental droplet gasification rates and liquid surface temperatures over a range of conditions. The experimental portion of the investigation included measurements of surface temperatures and gasification rates for porous spheres supported in a flowing combustion gas stream leaving a burner. Data was obtained for the pressure range 1-40 atm.

A number of theories were compared with these experimental results. The analysis involved the use of a spherically symmetric model for the gasification rate in the absence of convection, in conjunction with a multiplicative correction for the effect of convection, following a suggestion given in Ref. 4. The gas phase model of the combustion process involved a number of variable property treatments including; variable property-variable specific heat, variable property-constant specific heat and constant property versions. Phase equilibrium at the liquid surface was computed by convectional low pressure models (neglecting gas solubility and high pressure Poynting corrections) as well as a high pressure version for characteristics near the critical point, developed by Prausnitz and Chueh.⁵

The multiplicative correction has the form

$$\dot{n}/\dot{n}_0 = 1 + 0.278 \text{Re}^{1/2} \text{Pr}^{1/3} (1 + 1.237 \text{Re}^{-1} \text{Pr}^{-4/3})^{-1/2}$$

where

\dot{n} = convective burning rate

\dot{n}_0 = burning rate with no convection

Re = Reynolds number

Pr = Prandtl number

Following the suggestion of Ref. 4, the work in Ref. 1 employed approach conditions to evaluate properties in this expression.

Comparison between the various gas phase models indicated little difference in results as long as any assumed constant property was evaluated at an arithmetic average condition. The gasification rate predictions of the low and high pressure models were also essentially the same, with the exception that the high pressure model predicts a higher pressure for critical combustion. The overall results were not uniformly good, however, with errors ranging up to 50% between predicted and measured gasification rates. Agreement was generally poorest for high molecular weight hydrocarbons at low ambient oxidizer concentrations.

During the present report period, this comparison was extended to include further measurements of droplet gasification rates in combustion gas environments (2). Table 1 summarizes the range of test conditions for these two studies.

In addition to the use of approach conditions in the convection correlation, a second method was considered based on average conditions in the flow field around a droplet. Eisenklam, et al.⁶ have suggested a complex procedure for selecting average properties in a convection correlation. The method of Ref. 6, however, does not have correct asymptotic properties at low ambient oxidizer concentrations and it was not considered. For most fuels, the stoichiometry is such that the flame zone is located toward the outside of the flow field around the droplet. This is particularly the case at low ambient oxidizer concentrations. Therefore, based on this observation, properties in the convection correction were selected at average conditions between the flame and the drop surfaces since this region comprises the bulk of the flow field. The average taken is based upon the average temperature and composition in the region. The average mixture properties are computed as described in Ref. 1.

Some comparisons between predicted and measured gasification rates are shown in Figs. 1 and 2. Other examples may be found in Ref. 7. The rate of gasification has been normalized by the convection correction so that a range of test conditions can be shown on a single plot. Two sets of data are shown, one set normalized by the convection correction for approach conditions (darkened symbols), the other set using average conditions (open symbols). The theoretical curve is based upon a variable property-variable specific heat model of the combustion process in conjunction with both low and high pressure phase equilibrium models (1). Notably, the gasification rate prediction of these two models is essentially the same in the region in which they overlap (Fig. 2).

In general, the use of average conditions in the convection correction results in a better prediction of the gasification rate. The improvement is greatest for high molecular weight hydrocarbons at low ambient oxygen concentrations (lowest curve on Fig. 2). At higher ambient oxygen concentrations there is less difference between the two methods. This occurs since the approach temperature is a better approximation of the average of the droplet and flame temperature under these conditions.

Measured and predicted burning rates are compared over the entire data range in Fig. 3. The data points shown involve the use of approach conditions in the convection correction. In order to avoid cluttering the

Table I
Summary of Droplet Combustion Test Conditions

	Present	Faeth and Lazar ²
Test Method	porous sphere	suspended droplet
Ambient gas temperature (°K)	600-1500	1660-2530
Ambient oxygen conc. (mole %)	0-13.5	0-41.8
Pressure (atm)	1-40	1
Diameter (cm)	0.95	0.11
Approach Reynolds number	40-680	1.3-2.2

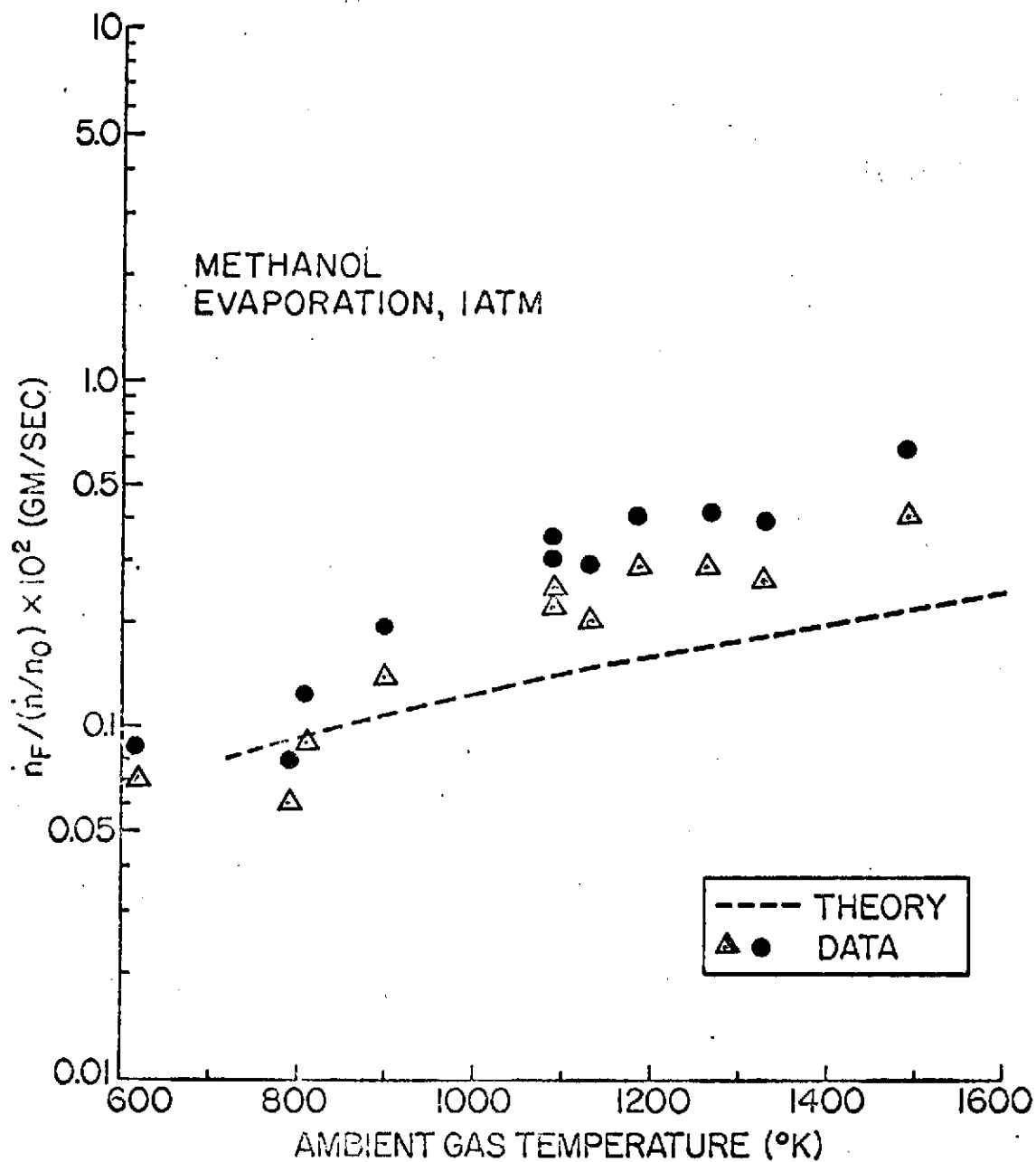


Figure 1 Evaporation rate of methanol as a function of ambient temperature at atmospheric pressure. Approach Reynolds number range 46-174. Approach convection correction-darkened symbols; averaged convection correction-open symbols.

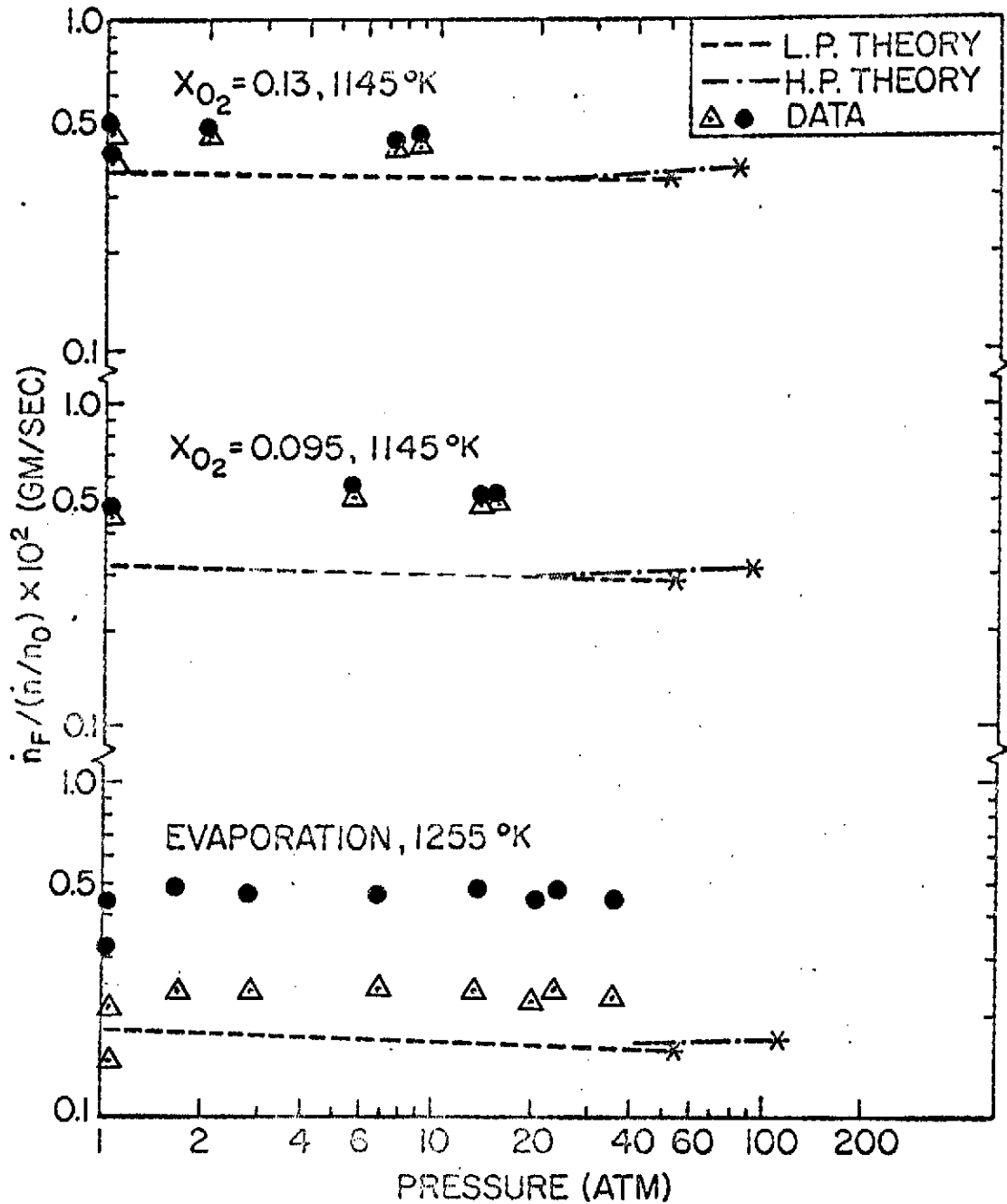


Figure 2 Gasification rates of n-heptane as a function of pressure for various ambient oxygen concentrations. Approach Reynolds number range 66-672. Approach convection correction-darkened symbols; averaged convection correction-open symbols.

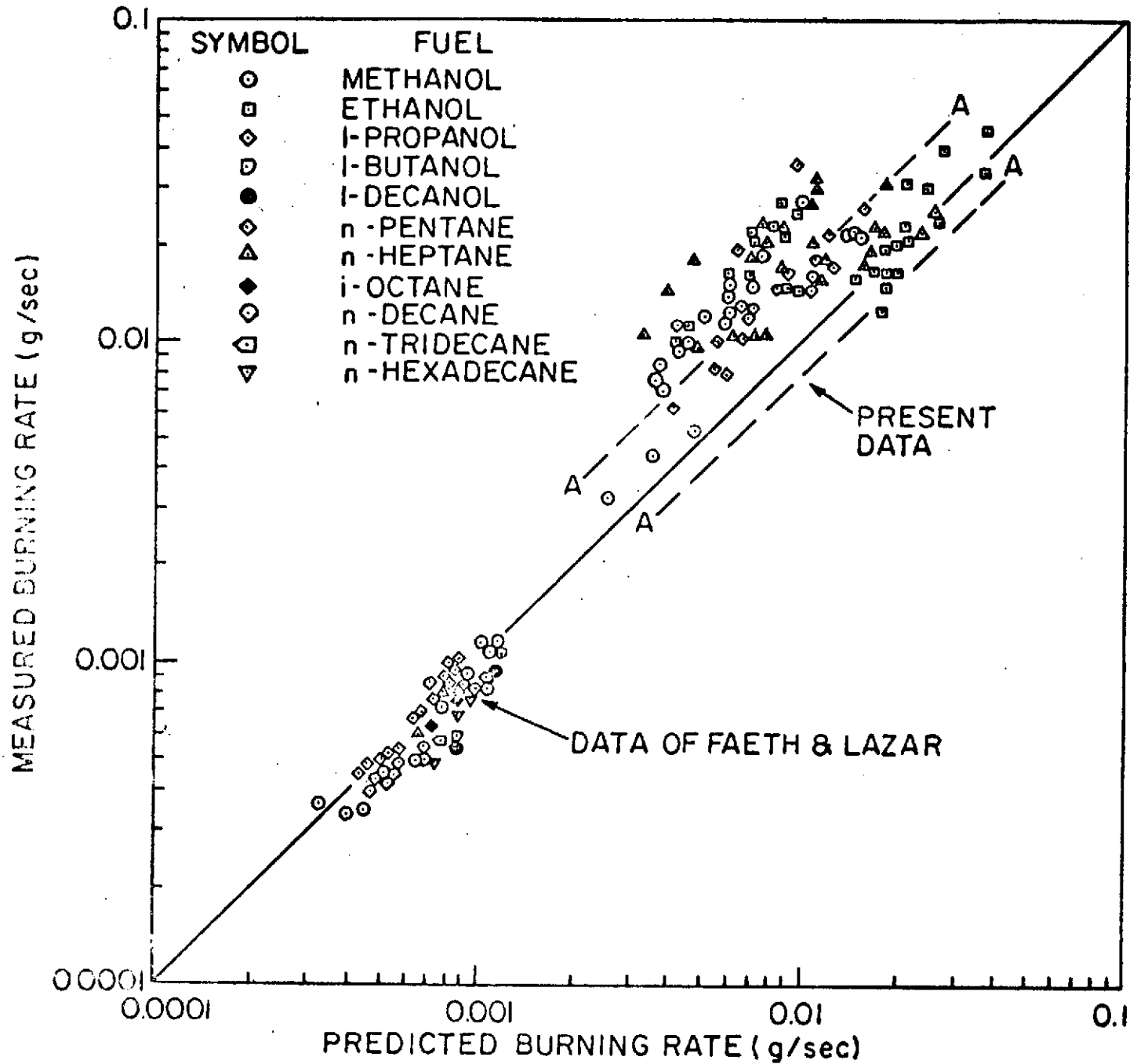


Figure 3 Overall comparison of theoretical and experimental gasification rates in combustion gas environments. Lines A-A are data bounds when average properties are used in the convection correction.

figure, the data using average properties in the convection correction are not shown individually. The bounds using the data of Ref. 1, with this latter procedure, are shown by the lines A-A. In the case of the measurements of Faeth and Lazar (2), the two procedures cannot be distinguished due to the low Reynolds numbers of these tests (Table 1).

Use of the averaged convection correction gave average differences between theory and experiment of $\pm 30\%$, with maximum discrepancies ranging up to 70%. The use of approach conditions gives poorer results, particularly for the high Reynolds number conditions of the present tests. Finally, the present procedure for averaging is superior to that suggested in Ref. 6, since the method is continuous as the ambient oxidizer concentration approaches zero.

2.3 Intermediate Pressure Model

The low and high pressure phase equilibrium models have been found to represent surface conditions adequately when the ambient pressure is less than or greater than half the pressure required for critical combustion respectively. This is illustrated in Figs. 4 and 5, taken from Refs. 8 and 9.

A characteristic of the two models, illustrated in Figs. 4 and 5, is that they do not merge at low pressures. This occurs since the Prausnitz and Chueh⁵ model is adjusted to give a good representation of conditions near the critical mixing point and fails to present liquid properties adequately at lower pressures, where the conventional models are accurate.

These results indicate the desirability of considering an intermediate pressure model that would provide a continuous transition between the two currently available versions. Since models in this region can be founded on a larger data base than the high pressure versions, they can provide more accurate predictions of high pressure phenomena. Since they formally merge with the low pressure versions, the intermediate pressure models give information on the limit of usefulness for the simpler low pressure models. Under combustion chamber conditions, the loss of surface tension near the critical point results in shattering of the droplet, therefore, the intermediate pressure versions are likely to provide information over the bulk of the range where droplet combustion, via an envelope flame model, actually exists. Finally, the intermediate pressure models provide a good estimation of phase equilibria for complex hydrocarbon mixtures and thus have potentially greater usefulness for practical fuel types (as opposed to pure hydrocarbons).

The introduction of a new phase equilibrium model does not require a change in the theoretical treatment of the gas phase. In fact, the results to date indicate that the present gas phase model is adequate within the regimes pertinent to the low and high pressure phase equilibrium models (Fig. 2 for example).

Of the various intermediate pressure models that could be used, the method outlined by Prausnitz, et al.¹⁰ has been selected for investigation. This procedure is well documented, and can be conveniently related to the current high pressure version. The detailed description of this model may be found in Ref. 10, in the following only a brief description will be given to indicate the main features of the method.

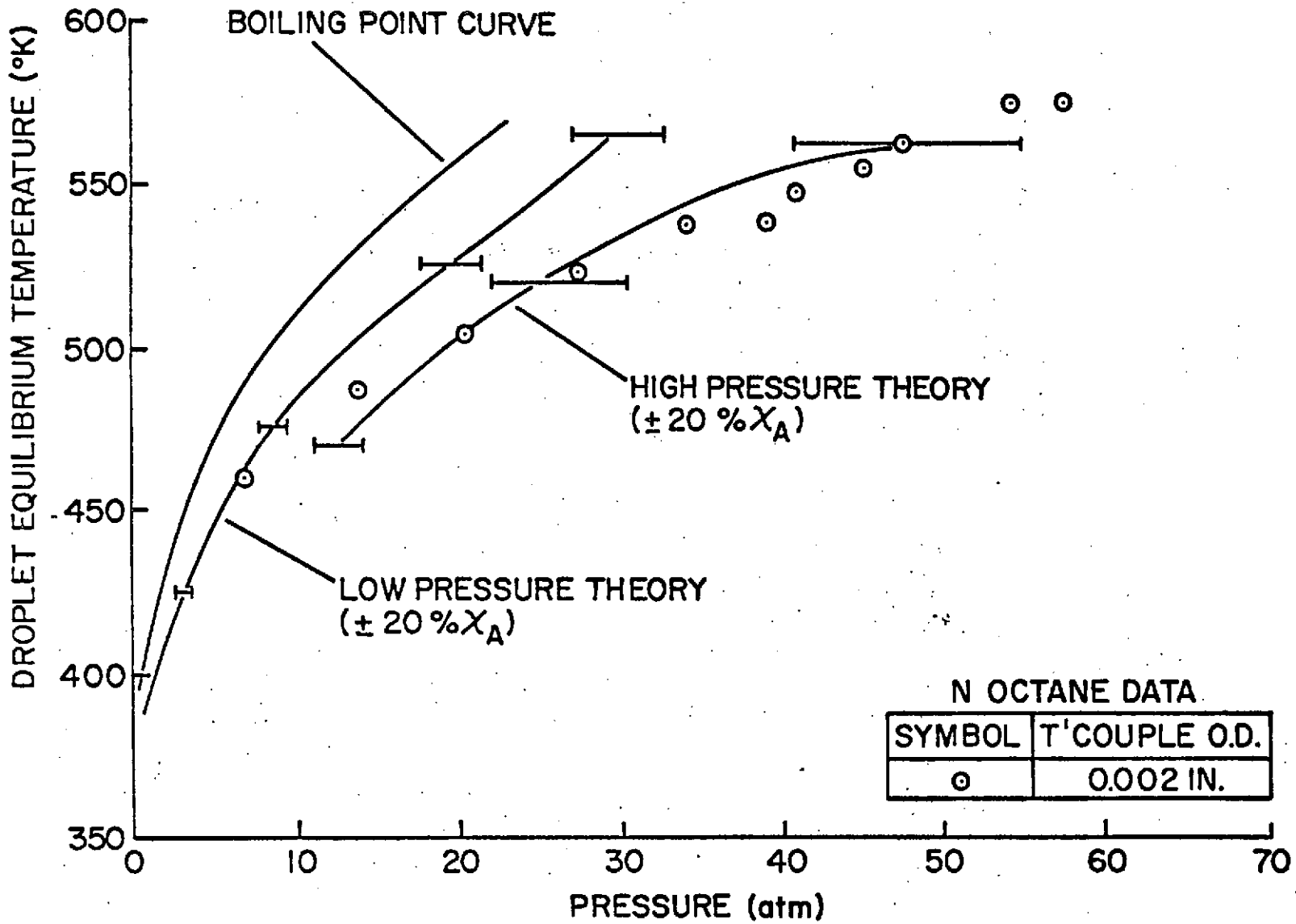


Figure 4 Liquid Surface Temperatures as a Function of Pressure for the Droplet Combustion Experiments of Ref. 8.

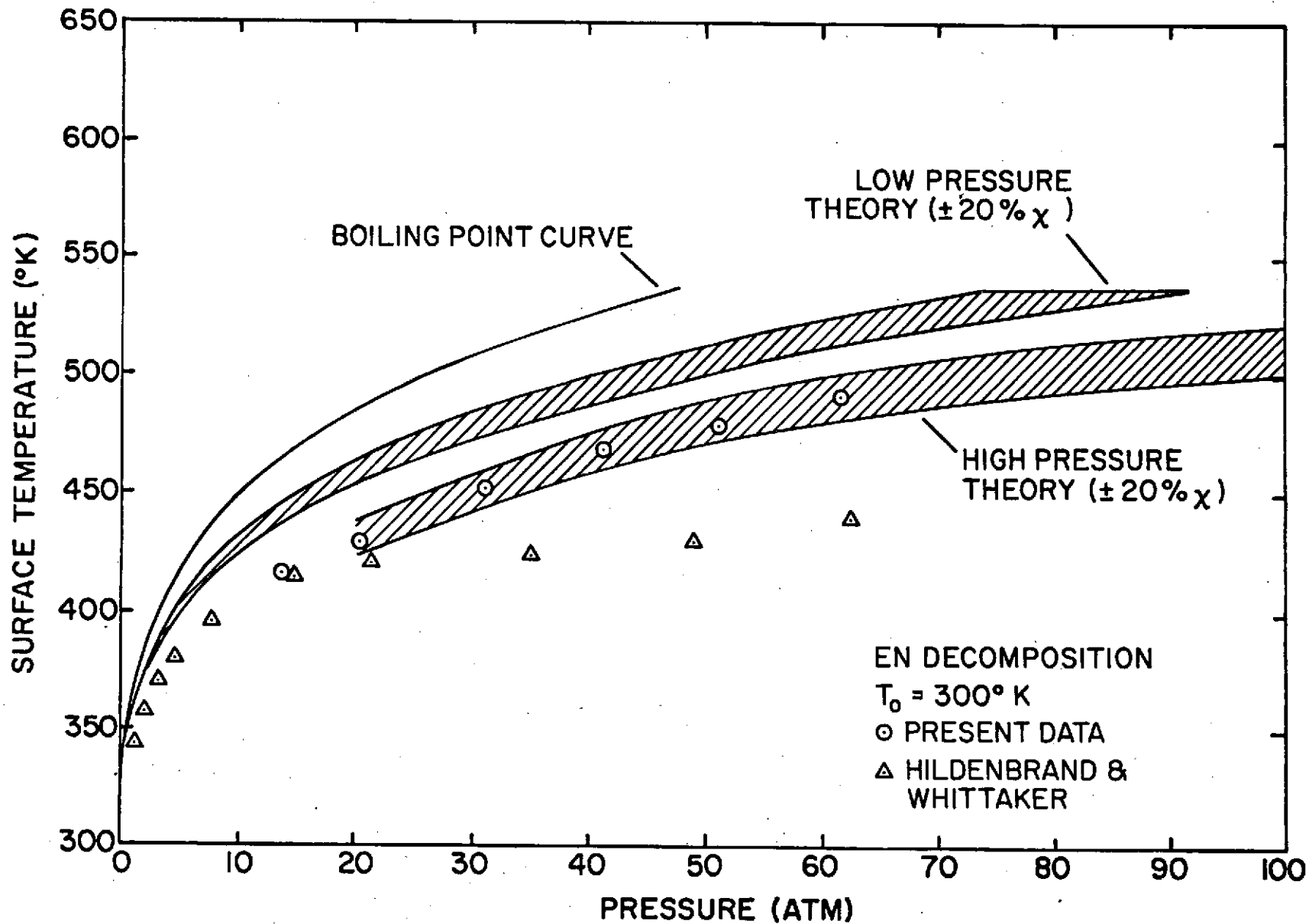


Figure 5 Liquid Surface Temperatures as a Function of Pressure for the Strand Combustion Experiments of Ref. 9.

For two phases to be in equilibrium, the total temperature and pressure must be equal in both phases, and the fugacity of each species in the system must be the same in both phases.

In the gas phase the fugacity, $f_i^V = Y_i \phi_i p$

where p is the total pressure, Y_i is the gas phase mole fraction of i and ϕ_i is the fugacity coefficient of i . The model computes the fugacity coefficient by the use of virial equation of state, taken to second order. The second virial coefficient is correlated in terms of individual and binary coefficients, which can be corrected for the presence of polar compounds in the system.

In the liquid phase, the fugacity is given by $f_i^L = x_i \gamma_i f_i^{ol}$

where x_i is the liquid phase mole fraction, γ_i is the activity coefficient and f_i^{ol} is the fugacity in a reference state. The reference state for a condensable component (one that is ordinarily a liquid at the temperature of the mixture) is the fugacity of the pure liquid. If the mixture temperature is higher than the critical temperature of the component, Henry's constant is used as the reference fugacity. Wilson's equation is used to evaluate of activity coefficient in both cases. This equation provides proper temperature dependence, and can be used for multicomponent mixtures while only requiring parameters obtainable from binary mixture data. The equation is also suitable for polar compounds.

With correlations available for the gas and liquid phase fugacities, calorimetric quantities such as heats of vaporization can be determined as described in Ref. 1. With these results in hand, the phase equilibrium model and the gas phase model can be solved simultaneously to yield liquid surface temperature predictions for comparison with the experimental results. This requires physical constants for the pure species (which are available), Wilson parameters, and Henry's constants. The latter quantities are available in some cases, must be fitted from binary data (if this exists), or must be estimated. Reference 10 discusses various procedures for determining these quantities.

At the present time, the computer program for the intermediate pressure model is being checked on the computer. The necessary property values for the correlation are being determined from the literature. When this work is completed, liquid surface temperatures will be predicted for the body of data available from earlier measurements (1, 2, 7, 8, 9, 11). The intermediate pressure model should overlap the range of validity of the high pressure model, allowing a check of the predictions of the two methods.

2.4 Summary

Work in the area of high pressure fuel droplet combustion has involved overall comparison of experimental and theoretical liquid surface temperatures and gasification rates in combustion gas environments. Predicted results are relatively independent of the gas phase model (when appropriate average properties are chosen). Using a convection correction with average properties between the droplet surface and the flame provides predictions within $\pm 30\%$ of measured values for typical combustion chamber conditions.

The low pressure phase equilibrium model is adequate for predicting liquid surface properties at total pressures less than half the pressure required for critical combustion. The high pressure model is more adequate at pressures approaching the critical combustion condition.

Work has been initiated on the development of an intermediate pressure phase equilibrium model, to provide a continuous transition between the present low and high pressure versions. This work should be concluded in the next report period.

3. Combustion Response of Monopropellant Droplets

3.1 Introduction

The objective of this phase of the investigation involves the determination of the open-loop combustion response of monopropellant droplets to imposed pressure oscillations. Knowledge of the frequency ranges where the combustion response is maximum, allows the designer either to adjust combustion geometry to avoid having characteristic chamber frequencies in this region or provide damping tuned to this frequency range.

The present work is a continuation of earlier efforts on obtaining a theoretical and experimental comparison for the response of a burning monopropellant strand to imposed pressure oscillations.³ Using these findings as a basis, current activities involve examination of the more practical case of droplet combustion. By utilizing a model generally substantiated by strand combustion results, this step to the droplet combustion case can be approached with some confidence.

Earlier work on the response of droplets has been confined to consideration of evaporation or bipropellant combustion.¹² Therefore, the present investigation should provide new information on the response characteristics of liquid fuels.

In the case of liquid strand combustion, for a given fuel, the frequency response curve changes only as the mean pressure is varied.³ For monopropellant droplets, however, droplet size also influences the process introducing a new parameter to the problem. Going from large droplets to small ones, the reaction zone becomes more influenced by curvature, and lies at proportionately greater distances from the surface for the small droplets.¹³ This implies that large droplets (where the reaction zone is close to the surface) behave somewhat like strands, while small droplets behave somewhat like evaporating droplets without reaction. Therefore, the present work provides information in the branch region limited on both sides by earlier results.

Initial work on this portion of the investigation involved, first of all, direct consideration of the large droplet limit in the context of the earlier strand combustion model. Then, using parameters determined in Ref. 3, the transient analysis is recast into a form appropriate for droplet combustion.

The above approach is limited to a frequency regime where the characteristic time of oscillation is small in comparison to the droplet lifetime. At low frequencies, a different procedure must be used, more analogous to the

vaporization response calculations based upon droplet lifetime (12, 14, 15). At this limit, the gas phase is essentially quasisteady providing a substantial simplification of the analysis. This approach can also be linked to the more complete perturbation analysis at the limit of a quasisteady gas phase. Therefore, the analysis treats these cases in a unified manner.

3.2 Large Droplet Limit

A burning liquid strand, itself, is analogous to a segment of an infinitely large liquid droplet. This analogy persists for a range of droplet sizes, allowing direct use of the results of Ref. 3 in this "large droplet" regime.

The actual size range of the "large droplet" regime will be considered later. In general terms, this is a condition where the reaction zone is close to the surface. For droplets of this type, ignition occurs before the bulk liquid has heated to any degree, and there are temperature gradients in the liquid phase.¹⁶⁻¹⁸ Since the reaction zone is close to the surface, the gas phase combustion process is largely uninfluenced by forced convection (unless very massive convection is present).^{13,16} In this situation, the combustion process is completely analogous to liquid strand combustion.

As an example of typical response characteristics, Fig. 6 shows the response for a hydrazine strand.³ The response is given as the real part of the acoustic admittance as a function of the dimensionless frequency of the imposed pressure oscillations. This parameter is equivalent to the response parameters defined in Ref. 12 for liquid fuel combustion, at the large droplet limit.

With increasing frequency, two positive peaks are observed in the acoustic admittance plot. The first peak occurs near the characteristic frequency of the thermal wave in the liquid phase, and is a result of the interaction between the combustion process and liquid phase transient effects. The second peak occurs at frequencies near the characteristic frequency of the gas phase thermal wave, and is a result of interaction between the combustion process and gas phase transient effects.

Combustion instability is usually associated with values of the real part of the acoustic admittance greater than a value on the order of unity.¹² Table 2 summarizes the frequency ranges where this criteria is satisfied for the results of Fig. 6. The results have been converted to dimensional form with the two frequency ranges corresponding to the liquid and gas phase transient regimes. At atmospheric pressure, only the gas phase transient range has sufficient amplification to drive instability, while at pressures greater than 10 atm., both regimes are of significance.

Typical frequency ranges for combustion instability and typical sizes for large droplets must be considered in order to relate the findings of Table 2 to practical combustion chambers. Combustion instability is usually associated with the frequency range 500-30,000 Hz.¹² At low pressures, Table 2, indicates that this range would involve gas phase transient effects; while for pressures greater than 10 atm. interaction of the combustion process with the liquid phase thermal wave is the more significant phenomena. These findings suggest that while the use of a quasisteady gas phase assumption at low pressures might be adequate for mean burning characteristics of monopropellants, potentially important contributions to the combustion response can be overlooked with this approach.

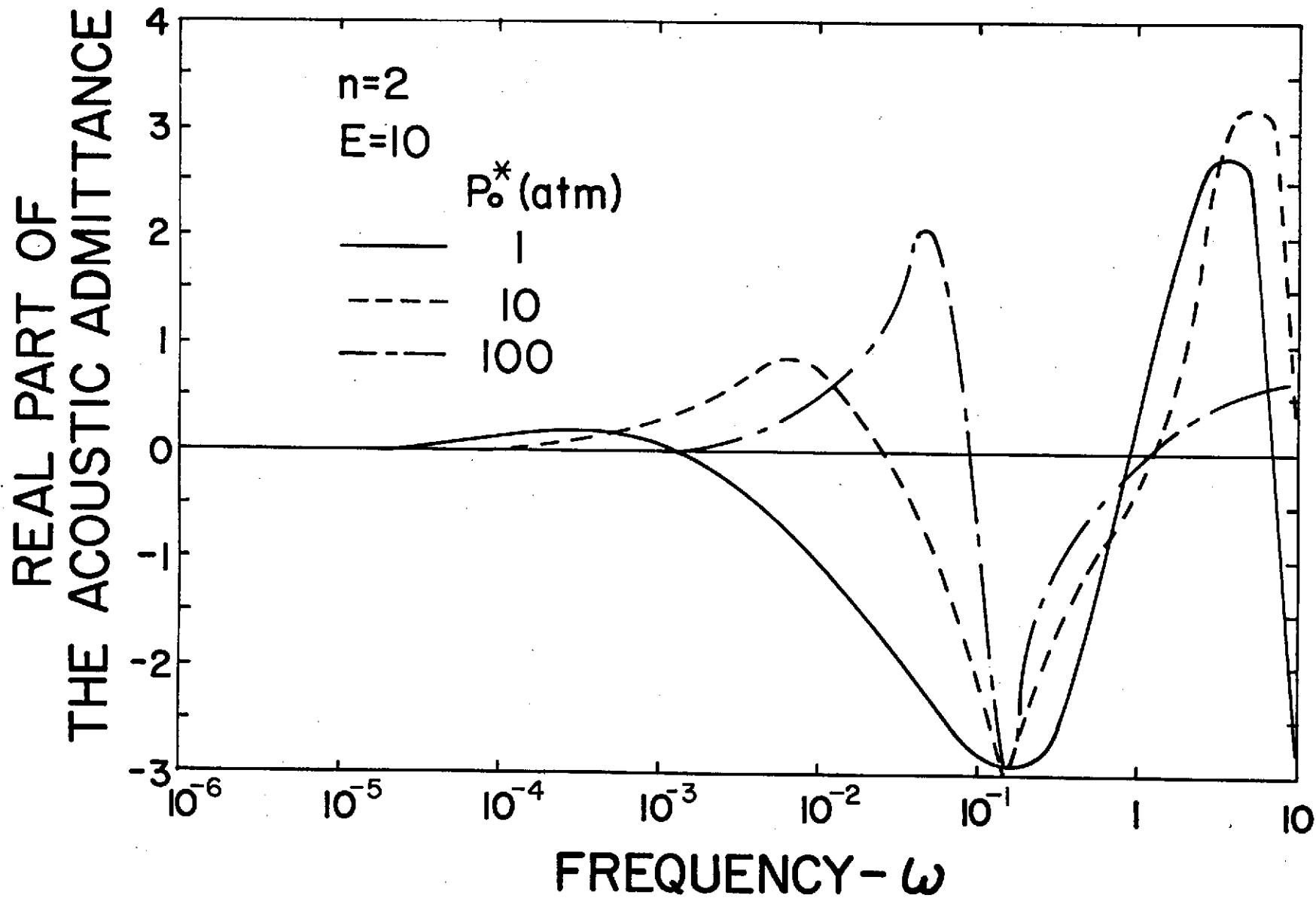


Figure 6 Computed Real Part of the Acoustic Admittance as a Function of Frequency and Pressure for Hydrazine.

Table 2
Critical Frequency Ranges for Hydrazine
Strand Combustion

Mean Pressure (atm)	Liquid Transient Range (HZ)	Gas Transient Range (HZ)
1	-	300-1500
10	approx. 15	4500-21500
100	450-1650	>225,000

The droplet size appropriate to the "large droplet" limit can be examined by estimating of the position of the reaction zone. Spalding's theory of mono-propellant droplet combustion (as presented in Ref. 19) provides a convenient approach to this problem when strand combustion rates are available. From this theory, it can be shown that the dimensionless flame position is given by (see Ref. 19 for notation)

$$\sigma_c^2 = (r_c/r_e)^2 = [2 + \Gamma + (\Gamma^2 + 4 \Gamma)^{1/2}] / 2 \Gamma$$

where

$$\rho_e v_e d_e c_p / \Gamma = (1 + \theta_e) \lambda_c \ln [1 + (1 - \theta_e) / \delta]$$

$$\theta_e = T_e / T_c$$

$$\delta = L / c_p T_c$$

For hydrazine, at pressures greater than atmospheric pressure, the liquid regression rate is given by³

$$v_e = 0.01254 p$$

where v_e is in cm/sec and p is in atmospheres.

Using property values for hydrazine given in Ref. 3, the droplet size can be computed for various flame positions and pressures. These results are given in Table 3 for dimensionless flame positions of 1.1 and 2.0.

In Table 3, for $\sigma_c = 1.1$ the decomposition flame is only 10% of the droplet radius away from the liquid surface. Droplets larger than the values listed in Table 3 for this σ_c should behave as "large droplets" (this estimation is preliminary, however, pending the results of the next phase of the investigation). Significantly, at the higher pressures, the "large droplet" regime covers the range of droplet sizes usually encountered in rocket engine applications. This indicates that the magnitude of the response (Fig. 6), the frequency range (Table 2) and the droplet size (Table 3) are all commensurate with the requirements for combustion instability under rocket engine conditions.

In Table 3, for $\sigma_c = 2$, the flame is located relatively far from the droplet and there is only weak interaction between the gasification of the liquid and the decomposition flame. Judging from earlier analyses of droplet evaporation and combustion response under these conditions,¹² the liquid transient response is likely to be much reduced at these conditions. The transient gas phase response, however, could still contribute at these conditions. Therefore, at low pressures, the unsteady gas phase may still be an important factor.

The drop size range between the two limits shown in Table 3 is a branch region where the liquid phase response should be increasing toward the large droplet limit. This clearly comprises a significant technological range of droplet sizes, indicating the importance of considering actual droplet response as opposed to just the large droplet limit. This, coupled with the possible importance of gas phase transient effects for small droplets at low pressures,

Table 3
Hydrazine Droplet Sizes as a Function of Flame
Position and Pressure

Pressure	Droplet Diameter (Microns)	
	$\sigma_c = 1.1$	$\sigma_c = 2.0$
1	5250	290
10	525	29.0
100	52.5	2.9

provides motivation for the more detailed analysis of droplet response considered in the next section.

3.3 Droplet Response Analysis

3.3.1 Description and Assumptions of the Model

The previous work has suggested the need for specific examination of the response of burning droplets. Since response is sought, as opposed to droplet lifetime calculations, the possible importance of gas phase transient effects must be considered. The previous work on strand combustion response has been substantiated by experiment, therefore, the present theoretical effort to extend the results to droplets can be approached with some confidence.

The configuration under consideration involves a droplet that is burning in the absence of convection, yielding a spherically symmetric flow field. While convection is important under actual combustion chamber conditions, there is evidence to indicate that the region where the droplet has a low (or zero) relative velocity with respect to the ambient gas is a very critical zone in determining combustion instability characteristics.¹² For simple evaporation without decomposition, the response due to velocity effects has been found to be quite low.²⁰ In addition, the decomposition process near the droplet surface reduces the influence of convection over a fairly wide range of conditions.^{13,16} This occurs since convection only influences the process when the outer edge of the flow field interacts with the reaction zone, a situation that is limited to very weak reactivity or very high Reynolds numbers. Therefore, neglecting convection for monopropellant droplets puts fewer limitations on the practicality of the calculations, than would be the case for bipropellants.

Similar to earlier response studies,^{3,20} the ambient pressure is assumed to be oscillating with a wavelength that is long in comparison to the dimensions of the combustion field of the droplet. The period of oscillation, however, is assumed to be short in comparison to the total droplet lifetime so that consideration does not have to be given to large changes in the position of the surface during a pressure oscillation. This assumption allows the analysis to proceed while only examining oscillatory solutions. The low frequency regime where this breaks down will be discussed later (this low frequency regime is largely associated with the range of frequencies where both liquid and gas phases are quasisteady).

Since the combustion rate of monopropellant droplets is much higher than bipropellants, the usual assumption of a constant liquid phase temperature (in the zero order) is less valid than for bipropellants. Therefore, the presence of mean liquid phase temperature gradients must be considered in the analysis. Examination of constant mean temperatures can be made, in order to include the conventional steady combustion model, by equating the bulk liquid temperature to the wet bulb temperature at a given pressure.

A sketch of the theoretical model is shown in Fig. 7. Notation may be found in Table 4. The process is examined at an instant of time when the droplet radius is r_g . Formally, this radius is taken to be fixed so that the mass flux of fuel is time varying. This actually corresponds to porous

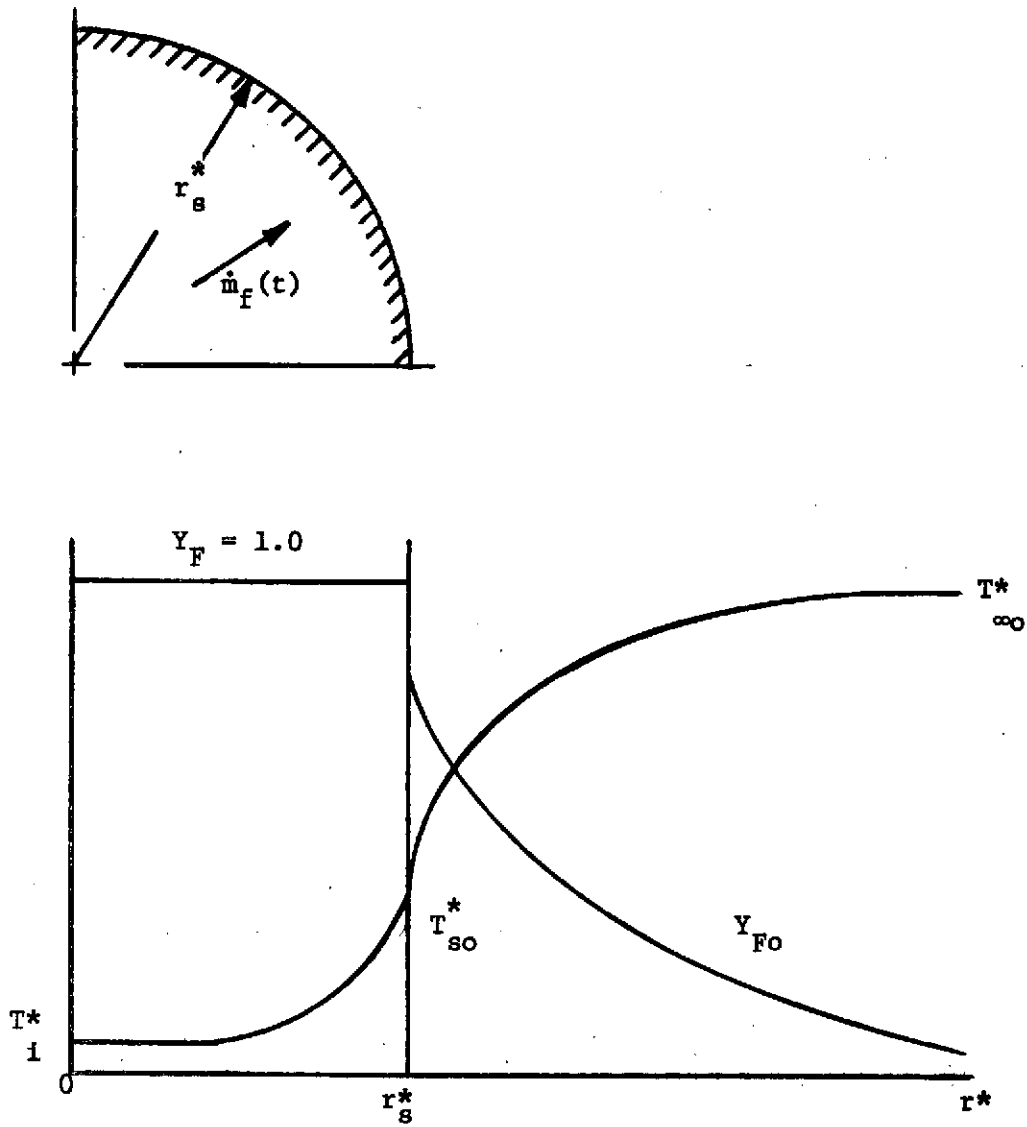


Figure 7 Sketch of the Droplet Combustion Response Model.

TABLE 4
Notation for Open-Loop Response Analysis

<u>Symbol</u>	<u>Description</u>
a	vapor pressure parameter, Eq. (21)
A	parameter, Eq. (11)
B	preexponential factor
C_p	specific heat
D	binary diffusivity
E	activation energy
h_i^o	heat of formation
i	$\sqrt{-1}$
L	heat of vaporization, Eq. (21)
L_f	vapor pressure parameter, Eq. (21)
\dot{m}	mass flow per unit solid angle
M	molecular weight
n	reaction order, Eq. (10)
p	pressure
q	energy of reaction
q_s	liquid phase heat flux, Eq. (58)
r	radial distance
R	gas constant
t	time
T	temperature
v_r	radial velocity
w	reaction rate
Y_i	mass fraction of species i
α	thermal diffusivity
β	parameter, Eq. (21)
γ	specific heat ratio
Γ	parameter, Eq. (55)
δ	reaction parameter, Eq. (10)
δ_f	parameter, Eq. (4)
ϵ	amplitude of oscillatory pressure, Eq. (29)
θ	combined variable, Eq. (23)

λ	thermal conductivity
ν_1', ν_1''	stoichiometric parameters, Eq. (5)
ν_1	parameter, Eq. (9)
ρ	density
σ	parameter, Eq. (69)
ϕ	parameter, Eq. (66)
ψ	parameter, Eq. (52)
ω	frequency
ω_s	frequency for strand case, Eq. (53)

Subscripts

f	liquid
F	fuel
i	center of droplet
s	liquid surface
o	steady state quantities
1	first order quantities
∞	ambient conditions

Superscripts

*	dimensional quantities
---	------------------------

sphere combustion, however, the two cases are equivalent as long as the density in the liquid phase is large compared to that of the gas phase and the period of oscillation is small in comparison to the lifetime of the droplet. When this is true, the motion of the surface with respect to the mean surface position is negligible and can be ignored. Exceptions to this assumption arise near the critical point and the present analysis is not valid in this regime. (Several other aspects of the model would also have to be modified in order to consider near critical conditions). The response portion of the analysis is invalid at frequencies having an oscillation period comparable to the lifetime of the droplet.

For generality, gas phase transient effects are included in the model, since results discussed earlier indicate that could be important at low pressures. The effect of variable properties are also included, so that the model is equivalent to the earlier strand combustion analysis (3).

The remaining assumptions of the analysis are similar to those of Ref. 3. They are as follows:

1. The process is spherically symmetric with a Mach number much less than unity and negligible body forces. Inertial and viscous terms in the momentum equation are neglected.
2. The reaction process is premixed and laminar. A one-step, irreversible chemical reaction takes place in the gas phase and any time lags associated with the chemical reaction itself are negligible, i.e. the chemical reaction is locally quasisteady and obeys an Arrhenius equation valid under steady state conditions. Chemical reaction is neglected in the liquid phase.
3. Radiation heat transfer is neglected.
4. The gas phase is taken to be an ideal gas and the Lewis number is assumed to be unity.
5. All gas diffusion coefficients are equal, all molecular weights are equal, all gas phase specific heats are equal and constant, the gas phase thermal conductivity is independent of composition and varies linearly with temperature, and the liquid is composed of a single chemical species having constant properties.
6. The combustion products are assumed to be insoluble in the liquid phase and the gas phase fuel mass fraction at the liquid surface is given by the Clausius - Clapeyron equation. As in the case of the gas phase reaction, the equilibrium at the surface is assumed to occur rapidly in comparison to other transient effects in the system.
7. The wavelength of any periodic pressure disturbance is assumed to be long compared with the diameter of the zone involving active combustion. Consideration of the momentum equation, along with Assumption 1, then implies that pressure is only a function of time.

A discussion of the applicability of these assumptions is provided in Ref. 3.

3.3.2 Governing Equations

The notation for the following analysis is provided in Table 4. In order to simplify notation, define the following dimensionless variables:

$$r = r^*/r_s^* \quad t = t^* \lambda_{\infty 0}^*/\rho_{\infty 0}^* C_p^* r_s^{*2}$$

$$v_r = v_r^* \rho_{\infty 0}^* C_p^* r_s^*/\lambda_{\infty 0}^* \quad \dot{m} = \dot{m}^* C_p^*/r_s^* \lambda_{\infty 0}^* \quad (1)$$

$$T = T^*/T_{\infty 0}^* \quad p = p^*/p_0^* \quad \rho = \rho^*/\rho_{\infty 0}^*$$

$$\lambda = \lambda^*/\lambda_{\infty 0}^* \quad D = D^*/D_{\infty 0}^*$$

where the subscript ∞_0 refers to a zero order (steady state) quantity, evaluated at infinity. The conservation equations are now considered in the liquid and gas phase, followed by the boundary conditions.

Liquid Phase $r < 1$

The equation of conservation of mass is

$$\rho_f r^2 v_{fr} = \dot{m}_f \quad (2)$$

where \dot{m}_f is the mass flow rate per unit solid angle and is only a function of time. Conservation of energy is

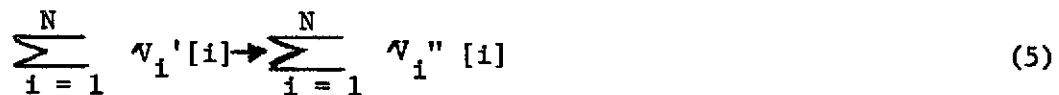
$$\frac{\partial T}{\partial t} + v_{fr} \frac{\partial T}{\partial r} = \frac{\delta_f}{r^2} \frac{\partial}{\partial r} \left(r^2 \frac{\partial T}{\partial r} \right) \quad (3)$$

where δ_f is the ratio of thermal diffusivities

$$\delta_f = \alpha_f/\alpha_{\infty 0} \quad (4)$$

Gas Phase $r > 1$

The stoichiometry of the one-step gas phase reaction is assumed to have the following form:



Overall conservation of mass in the gas phase is

$$\frac{\partial \rho}{\partial t} + \frac{1}{r^2} \frac{\partial}{\partial r} (\rho r^2 v_r) = 0 \quad (6)$$

It is also convenient to define a gas phase mass flow rate per unit solid angle, analogous to Eq. 2, as follows:

$$\dot{m} = \rho r^2 v_r \quad (7)$$

In this case, \dot{m} is a function of both radial distance and time.

Conservation of species becomes

$$\rho \left(\frac{\partial Y_i}{\partial t} + v_r \frac{\partial Y_i}{\partial r} \right) = \frac{1}{r^2} \frac{\partial}{\partial r} (r^2 \rho D \frac{\partial Y_i}{\partial r}) + v_i w, \quad i = 1, N \quad (8)$$

where

$$v_i = (v_i'' - v_i') / v_F' \quad (9)$$

$$w = A p^n T^{\delta-n} Y_F^n \exp(-E/T) \quad (10)$$

$$A = \frac{C_p^* B^* r_s^{*2} T_{\infty}^{*\delta}}{\lambda_{\infty}^*} \left[\frac{P_o}{M^* R^* T_{\infty}^*} \right]^n \quad (11)$$

and

$$E = E^* / R^* T_{\infty}^* \quad (12)$$

Finally, conservation of energy is

$$\rho \left(\frac{\partial T}{\partial t} + v_r \frac{\partial T}{\partial r} \right) = \frac{1}{r^2} \frac{\partial}{\partial r} (r^2 \lambda \frac{\partial T}{\partial r}) + \left(\frac{\gamma - 1}{\gamma} \right) \frac{dp}{dt} + q w \quad (13)$$

where

$$q = - \sum_{i=1}^N h_i^{*o} (v_i'' - v_i') / (v_F' C_p^* T_{\infty}^*) \quad (14)$$

is the dimensionless heat of reaction, and p is only a function of time.

The assumption of an ideal gas having a unity Lewis number and with thermal conductivity proportional to temperature; provides the following relationship between properties:

$$T = \lambda = \rho D = p/\rho \quad (15)$$

Boundary Conditions

Since the liquid is incompressible, it has a constant temperature at the origin

$$r = 0 \quad T = T_i \quad (16)$$

In the case of steady combustion at the wet bulb temperature of the droplet, T_i would be equal to the wet bulb temperature. However, since monopropellants have higher gasification rates than most bipropellants, cases exist where temperature gradients are present in the liquid phase throughout the lifetime of the droplet. Therefore, T_i is taken as a parameter for the analysis in order to investigate the effect of these gradients on the response.

Aside from continuity of temperature and pressure at the surface of the droplet, four other conditions must be satisfied. These may be summarized as follows:

$$r = 1$$

$$\rho_f v_{rf} = \rho v_r \quad (17)$$

$$\lambda_f \left. \frac{\partial T}{\partial r} \right|_{s-} = \lambda \left. \frac{\partial T}{\partial r} \right|_{s+} - \rho v_r [(1-\beta) T + L] \quad (18)$$

$$\rho D \left. \frac{\partial Y_F}{\partial r} \right|_{s+} = \rho v_r (Y_F - 1) \quad (19)$$

$$Y_F = \frac{a}{p} \exp(-L_f/T) \quad (20)$$

where

$$\begin{aligned} \beta &= C_f^*/C_p^* \\ L &= L^*/R^*T_{\infty 0}^* \\ a &= a^*/p_0^* \\ L_f &= L_f^*/RT_{\infty 0}^* \end{aligned} \quad (21)$$

Equation (17) represents conservation of mass at the surface. Equation (18) is the conservation of energy relationship, where the heat flux reaching the surface goes into the heat flux in the liquid phase and the heat of vaporization of the gasifying fuel. Equation (19) follows from the insolubility of the product species in the liquid phase which implies that the total mass flux of the non-fuel species must be zero at the surface of the droplet. Equation (20) is the Clausius-Clapeyron equation relating the fuel mass fraction to temperature at the surface. Formally, L_f and L should be equal, however, the vapor pressure curve of the fuel is often better represented by a value of L_f slightly different than that of the heat of vaporization so that provision has been made for this possibility. Far from the droplet, all the fuel is consumed and the temperature is independent of distance

$$r = \infty \quad Y_F = 0 \quad T = T(t) \quad (22)$$

where $T(t)$ is a known function depending upon the specified pressure variation.

3.3.3 Schvab-Zeldovich Transformation

The solution can be simplified by introducing a Schvab-Zeldovich variable based on the fuel mass fraction

$$\theta = q Y_F + T \quad (23)$$

In terms of this variable, Eq. (8) is replaced by

$$\rho \left(\frac{\partial \theta}{\partial t} + v_r \frac{\partial \theta}{\partial r} \right) = \frac{1}{r^2} \frac{\partial}{\partial r} \left(\lambda \frac{\partial \theta}{\partial r} \right) + \left(\frac{\gamma - 1}{\gamma} \right) \frac{dp}{dt} \quad (24)$$

Gas phase conservation of energy is unchanged, however, the reaction rate becomes

$$w = A q^{-n} p^n T^{\delta-n} (\theta - T)^n \exp(-E/T) \quad (25)$$

The boundary conditions at the liquid surface, Eqs. (19) - (20) are as follows:

$$r = 1,$$

$$\lambda \frac{\partial(\theta - T)}{\partial r} \Big|_{s+} = \rho v_r (\theta - T - q) \quad (26)$$

$$\theta - T = \frac{aq}{p} \exp(-L_f/T) \quad (27)$$

The boundary conditions far from the droplet become

$$r = \infty$$

$$\theta = T = T(t) \quad (28)$$

The remaining equations are unchanged.

3.3.4 Perturbation Analysis

Following the approach used in Ref. 3, a linear perturbation analysis is conducted. It is assumed that the pressure oscillates with small amplitude, ϵ , and the dependent variables are represented as follows:

$$\begin{aligned}
 p(t) &= 1 + \epsilon e^{i\omega t} \\
 T(r,t) &= T_0(r) + \epsilon T_1(r) e^{i\omega t} \\
 \theta(r,t) &= \theta_0(r) + \epsilon \theta_1(r) e^{i\omega t} \\
 \dot{m}(r,t) &= \dot{m}_0(r) + \epsilon \dot{m}_1(r) e^{i\omega t} \\
 \dot{m}_f(t) &= \dot{m}_{f0} + \epsilon \dot{m}_{f1} e^{i\omega t}
 \end{aligned} \tag{29}$$

Substituting Eqs. (29) into Eqs. (1-28), the resulting equations are separated into like powers of $\epsilon e^{i\omega t}$. Equation (15) is also employed in order to reduce the equations to forms involving only θ and T .

The zero order, steady state, equations are as follows:

$$\dot{m}_{f0} = \dot{m}_0 = \text{const} \tag{30}$$

In the liquid phase, $r \leq 1$

$$\frac{d}{dr} \left(r^2 \frac{dT_0}{dr} \right) - \frac{\dot{m}_{f0}}{\rho_f \delta_f} \frac{dT_0}{dr} = 0 \tag{31}$$

In the gas phase, $r > 1$

$$\frac{d}{dr} \left(r^2 T_0 \frac{d\theta_0}{dr} \right) - \dot{m}_0 \frac{d\theta_0}{dr} = 0 \tag{32}$$

$$\frac{d}{dr} \left(r^2 T_0 \frac{dT_0}{dr} \right) = \dot{m}_0 \frac{dT_0}{dr} + r^2 q^{1-n} A T_0^{\delta-n} (\theta_0 - T_0)^n \exp(-E/T_0) = 0 \tag{33}$$

The boundary conditions are:

$$r = 0 \quad T_0 = T_i \tag{34}$$

$r = 1,$

$$\lambda_f \left. \frac{dT_0}{dr} \right|_{s-} = T_0 \left. \frac{dT_0}{dr} \right|_{s+} - \dot{m}_0 [(1-\beta)T_0 + L] \tag{35}$$

$$T_0 \left. \frac{d(\theta_0 - T_0)}{dr} \right|_{s+} = \dot{m}_0 (\theta_0 - T_0 - q) \tag{36}$$

$$\theta_0 - T_0 = a q \exp(-L_f/T_0) \tag{37}$$

$$r = \infty, \quad \theta_0 = T_0 = 1 \tag{38}$$

The first order equations are as follows. In the liquid phase, $r \leq 1$

$$\dot{m}_{f1} = \text{const} \quad (39)$$

$$\frac{d}{dr} \left(r^2 \frac{dT_1}{dr} \right) - \frac{\dot{m}_{fo}}{\rho_f \delta_f} \frac{dT_1}{dr} - \frac{i\omega r^2}{\delta_f} T_1 = \frac{\dot{m}_{f1}}{\rho_f \delta_f} \frac{dT_o}{dr} \quad (40)$$

In the gas phase, $r > 1$

$$T_o^2 \frac{d\dot{m}_1}{dr} - i\omega r^2 T_1 = -i\omega r^2 T_o \quad (41)$$

$$\begin{aligned} T_o \frac{d}{dr} \left(r^2 T_o \frac{d\theta_1}{dr} \right) - \dot{m}_o T_o \frac{d\theta_1}{dr} - r^2 i\omega \theta_1 &= (\dot{m}_o T_1 + \dot{m}_1 T_o) \frac{d\theta_o}{dr} \\ - T_o \frac{d}{dr} \left(r^2 T_1 \frac{d\theta_o}{dr} \right) - T_1 \frac{d}{dr} \left(r^2 T_o \frac{d\theta_o}{dr} \right) - r^2 \left(\frac{\gamma-1}{\gamma} \right) i\omega T_o & \end{aligned} \quad (42)$$

$$\begin{aligned} T_o \frac{d}{dr} \left(r^2 T_o \frac{dT_1}{dr} \right) - \dot{m}_o T_o \frac{dT_1}{dr} - r^2 i\omega T_1 &= (\dot{m}_o T_1 + \dot{m}_1 T_o) \frac{dT_o}{dr} \\ - T_o \frac{d}{dr} \left(r^2 T_1 \frac{dT_o}{dr} \right) - T_1 \frac{d}{dr} \left(r^2 T_o \frac{dT_o}{dr} \right) - r^2 \left(\frac{\gamma-1}{\gamma} \right) i\omega T_o & \\ - r^2 q^{1-n} A T_o^{1+\delta-n} (\theta_o - T_o)^n \exp(-E/T_o) \left[n + (1+\delta-n) \frac{T_1}{T_o} \right. & \\ \left. + n \left(\frac{\theta_1 - T_o}{\theta_o - T_o} \right) + \frac{ET_1}{T_o^2} \right] & \end{aligned} \quad (43)$$

The boundary conditions on these equations are

$$r = 0 \quad T_1 = 0 \quad (44)$$

$$r = 1 \quad \dot{m}_{f1} = \dot{m}_1 \quad (45)$$

$$\lambda_f \left(\frac{dT_1}{dr} \right)_{s-} = T_o \left(\frac{dT_1}{dr} \right)_{s+} + T_1 \left(\frac{dT_o}{dr} \right)_{s+} - \dot{m}_o (1-\beta) T_1 - \dot{m}_1$$

$$[(1-\beta) T_o + L] \quad (46)$$

$$T_o \left(\frac{d(\theta_1 - T_1)}{dr} \right)_{s+} + T_1 \left(\frac{d(\theta_o - T_o)}{dr} \right)_{s+} = \dot{m}_o (\theta_1 - T_1) + \dot{m}_1 (\theta_o - T_o - q) \quad (47)$$

$$\theta_1 - T_1 = a q \exp \{ -L_f/T_o \} \left[\frac{L_f T_1}{T_o^2} - 1 \right] \quad (48)$$

From Eq. (28), θ_1 and T_1 must approach a constant value from the surface of the droplet. Solving Eq. (43) for large r it can be shown that

$$r = \infty \quad \theta_1 = T_1 = \frac{\gamma - 1}{\gamma} \quad (49)$$

which is the form for isentropic flow.

The solution of Eq. (31) can be obtained immediately for the boundary conditions $T_o = T_i$ at $r = 0$ and $T_o = T_{os}$ at $r = 1$, as follows:

$$\frac{T_o - T_i}{T_{os} - T_i} = \exp \left[\frac{\dot{m}_{fo}}{\rho_f \delta_f} \left(1 - \frac{1}{r}\right) \right] \quad (50)$$

Equation (50) provides an expression for the steady state temperature distribution in the liquid phase.

In the gas phase, Eq. (32) can also be integrated once without difficulty. Applying the boundary conditions at the droplet surface, Eq. (35) and (36), and determining the liquid phase temperature gradient from Eq. (50), yields

$$r^2 T_o \frac{d\psi_o}{dr} - \dot{m}_o \psi_o = 0 \quad (51)$$

where

$$\psi_o = \theta_o + (\lambda/\rho\delta)_f (T_{os} - T_i) + L - \beta T_{os} - q \quad (52)$$

In general, the solution of the remaining equations must be obtained numerically. For the zero order problem, Eqs. (33) and (51) must be integrated. There remain four boundary conditions that have not yet been used, among Eqs. (35)-(38). Three of these provide boundary conditions on the differential equations, the fourth determines the eigenvalue \dot{m}_o .

The first order equations, Eqs. (39)-(43), are linear, requiring at total of seven boundary conditions. Equations (44)-(49), plus the compatibility conditions at the liquid surface, $T_1 - T_{1s}$, provides eight boundary conditions. The extra boundary condition determines the eigenvalue \dot{m}_{f1} , which can be related to the response.

The solution of the entire system of equations, Eqs. (29)-(52), represents a formidable task, even on the computer. Numerical calculations along this line are currently in progress and the results will be reported later. Under certain circumstances, however, the computations can be simplified considerably. The formulation under these conditions will be undertaken in the following.

3.4 Quasisteady Gas Phase Analysis

3.4.1 General Analysis

Consideration of the strand combustion case in Ref. 3, indicated that transient

gas phase phenomena contributed to the combustion response when the strand dimensionless frequency, ω_s , was of order unity. The present dimensionless frequency is related to the earlier value as follows:

$$\omega = \left(\frac{\dot{m}_o^* C_p^* r_s^*{}^2}{\lambda_{\infty o}^*} \right) \omega_s \quad (53)$$

At high rates of reaction, the factor in parenthesis in Eq. (53) is a constant. This quantity can be evaluated from the hydrazine droplet combustion data of Ref. 21. The results indicate that at the limit of high reactivities, important gas phase transient effects should not be encountered for dimensionless frequencies less than 1000. In this region, the gas phase may be assumed to be quasisteady with all important transient effects confined to the liquid phase.

The quasisteady regime also encompasses the low frequency region where the time of oscillation is an appreciable fraction of the lifetime of the droplet and the previous perturbation analysis is invalid. Therefore, in developing relations for the quasisteady limit, an objective is to obtain a unified treatment both by perturbation analysis and eventually by droplet lifetime calculations.

In order to achieve these objectives, the gas phase is analyzed, neglecting time derivatives. The boundary conditions of the problem are the droplet surface temperature and the ambient conditions. With this information, the mass fraction of fuel at the surface is also known through the Clausius-Clapeyron equation. The desired results of the analysis are the heat and mass fluxes at the droplet surface. This information can then be used to determine both response and lifetime characteristics of the droplet.

The assumptions of the analysis are the same as in the earlier treatment, except for additionally neglecting gas phase transient effects. Under these assumptions, the conservation equations are as follows:

$$r^2 \rho v_r = \dot{m} \quad (54)$$

$$r^2 \lambda \frac{d\Gamma}{dr} - \dot{m} \Gamma = 0 \quad (55)$$

$$\frac{d}{dr} \left(r^2 \lambda \frac{dT}{dr} - \dot{m} T \right) + r^2 q_w = 0 \quad (56)$$

where

$$\Gamma = \theta + q_s + L - \beta T_s - q \quad (57)$$

$$q_s = \frac{\lambda_f}{\dot{m}} \left. \frac{dT}{dr} \right|_{s-} \quad (58)$$

The boundary conditions on these equations are

$$r = 1 \quad T = T_s \quad (59)$$

$$\theta = \theta_s = \frac{qa}{p} \exp(-L_f/T_s) + T_s \quad (60)$$

$$\lambda \frac{dT}{dr} \Big|_{s+} = \dot{m} [q_s + (1-\beta)T_s + L] \quad (61)$$

$r = \infty$

$$T = \theta = 1 \quad (62)$$

The definitions of θ , w , etc. are the same as before and Eq. (15) provides a representation of the physical properties. The mass flux per unit solid angle, \dot{m} , is a constant throughout the gas phase. The quantity q_s , defined in Eq. (58) is the heat flux to the liquid phase after the heat of vaporization requirements at the surface have been met.

Equations (55) and (56) must be integrated numerically in general. Given T_s and p , Eqs. (60) yields θ_s . The equations only require one additional boundary condition, Eqs. (61) and (62) provide three. Therefore, the additional boundary conditions determine the eigenvalues \dot{m} and q_s . In this manner, the solution of the equations determines the functions

$$\dot{m} = \dot{m}(p, T_s, A) \quad (63)$$

$$q_s = q_s(p, T_s, A) \quad (64)$$

where A carries the influence of droplet size.

3.4.2 Gas Phase Analysis for Small A

For very small droplets, the parameter A is small, and the effect of reaction can be neglected. At this limit, the droplet simply evaporates. The solution of the gas phase equations can be completed analytically under this conditions, as described in the following.

With A equal to zero, Eq. (56) may be integrated once, yielding the following after applying the boundary condition of Eq. (61).

$$r^2 \lambda \frac{d\phi}{dr} - \dot{m} \phi = 0 \quad (65)$$

where

$$\phi = T + q_s + L - \beta T_s \quad (66)$$

Eliminating spatial derivatives between Eqs. (55) and (65) and then integrating yields an expression for θ , as follows:

$$\frac{\theta + q_s + L - \beta T_s - q}{\theta_s + q_s + L - \beta T_s - q} = \frac{T + q_s + L - \beta T_s}{T_s + q_s + L - \beta T_s} \quad (67)$$

after applying the boundary condition at the droplet surface.

Equation (65) is also readily integrated. After applying the surface boundary conditions the following is obtained:

$$\dot{m} \left(1 - \frac{1}{r}\right) = T - T_s - \sigma \ln [(T+\sigma)/(T_s + \sigma)] \quad (68)$$

where

$$\sigma = q_s + L - \beta T_s \quad (69)$$

The eigenvalues, \dot{m} and q_s are determined by applying the outer boundary conditions, Eqs. (62), to Eqs. (67) and (68). This yields

$$\dot{m} = (1-T_s) - \sigma \ln [(1+\sigma)/(T_s + \sigma)] \quad (70)$$

$$q_s = q \left(\frac{1 - T_s}{\theta_s - T_s} \right) - (1-\beta T_s + L) \quad (71)$$

where it is recalled that

$$\theta_s = \frac{qa}{p} \exp(-L_f/T_s) + T_s \quad (60)$$

Equations (70), (71) and (60) provide the necessary transport parameters at the droplet surface. They represent analytical forms of Eqs. (63) and (64) at the limit of A equal to zero.

3.4.3 Perturbation Analysis

If the liquid phase equations are perturbed, Eq. (50) still represents the zero order solution. The steady state surface temperature is then related to the bulk liquid temperature, as follows:

$$q_{so} = \frac{\lambda_f}{\dot{m}_o} \left(\frac{dT_o}{dr} \right)_{s-} = \left(\frac{\lambda}{\rho \delta} \right)_f (T_{os} - T_i) \quad (72)$$

Therefore, given T_i and p , Eqs. (64) and (72) can be solved to yield T_{os} . The zero order gasification rate, \dot{m}_o , can then be obtained from Eq. (63).

The first order liquid phase equations are also unchanged from Eqs. (39) and (40). The boundary conditions, for a given value of A, are

$$r = 0 \quad T_1 = 0 \quad (73)$$

$$r = 1 \quad \dot{m}_{f1} = \dot{m}_1 \quad (74)$$

$$\lambda_f \left(\frac{dT_1}{dr} \right)_{s^-} = \dot{m}_o q_{s1} + \dot{m}_1 q_{s0} \quad (75)$$

where

$$\dot{m}_1 = \left(\frac{\partial \dot{m}}{\partial T_s} \right)_p T_{1s} + \left(\frac{\partial \dot{m}}{\partial p} \right)_{T_s} \quad (76)$$

$$q_{s1} = \left(\frac{\partial q_s}{\partial T_s} \right)_p T_{1s} + \left(\frac{\partial q_s}{\partial p} \right)_{T_s} \quad (77)$$

The derivatives in Eqs. (76) and (77) are known from the general gas phase solution, evaluated at T_{os} , p_o . Solution of Eq. (40), with the boundary conditions of Eqs. (73)-(77), allows the eigenvalue \dot{m}_1 to be determined.

When analytical forms are available, as is the case when $A = 0$ (Eqs. 70 and 71), the derivatives in Eqs. (76) and (77) can be determined exactly. For finite values of A , only numerical results are available for the functions represented by Eqs. (63) and (64). In this case, the derivatives can be determined from plotted numerical results using p and T_s alternately as parameters. This procedure essentially corresponds to the Zeldovich method (22), which has recently received some attention for the calculation of solid propellant combustion response (23-25). Unlike the solid propellant case, however, the present calculations must include droplet size as a parameter, through A .

At the present time, the quasisteady gas phase analysis has been programmed on the computer for the general case of any value of A . Calculations are also proceeding at the limit of small A . These numerical results will be completed in the next report period.

3.5 Summary

During this report period, results for burning liquid monopropellant strand have been applied directly to determine preliminary droplet response characteristics for large droplets. The generalized analysis has also been completed allowing for transient phenomena in both gas and liquid phases.

The system has also been analyzed at the limit of a quasisteady gas phase. In this case, simple analytical forms have been obtained, as well, at the limit of an evaporating droplet.

At the present time, calculations are in progress to determine the open loop response function for monopropellant droplets (12). Initially work is considering response under the limitations of a quasisteady gas phase. The transient gas phase response will follow after the simpler case has been considered. The results of these calculations will be presented in the next report period.

References

1. G. S. Canada, "High Pressure Combustion of Liquid Fuels," NASA CR-134540, January, 1974.
2. G. M. Faeth and R. S. Lazar, "Fuel Droplet Burning Rates in a Combustion Gas Environment," AIAA J., Vol. 9, No. 11, pp. 2165-2171, November, 1971.
3. C. B. Allison, "Burning Rate Response of Liquid Monopropellants to Imposed Pressure Oscillations," NASA CR-134541, January 1974.
4. Williams, F. A., Combustion Theory, Addison-Wesley, Reading, Massachusetts, pp. 56-57, 1965.
5. Prausnitz, J. M. and P. L. Chueh, Computer Calculations for High Pressure Vapor-Liquid Equilibria, Prentice-Hall, Englewood Cliffs, New Jersey, 1968.
6. Eisenklam, P., S. A. Arunachalam and J. A. Weston, "Evaporation Rates and Drag Resistance of Burning Drops," Eleventh Symposium (International) on Combustion, The Combustion Institute, Pittsburgh, pp. 715-728, 1967.
7. G. S. Canada and G. M. Faeth, "Combustion of Liquid Fuels in a Flowing Combustion Gas Environment," Fifteenth Symposium (International) on Combustion, Tokyo, August 1974.
8. R. S. Lazar and G. M. Faeth, "Bipropellant Droplet Combustion in the Vicinity of the Critical Point," Thirteenth Symposium (International) on Combustion, The Combustion Institute, Pittsburgh, Pennsylvania, pp. 743-753, 1971.
9. G. M. Faeth, "High Pressure Liquid Monopropellant Strand Combustion," Combustion and Flame, Vol. 18, No. 1, pp. 103-113, February 1972.
10. Prausnitz, et al., Computer Calculations for Multicomponent Vapor-Liquid Equilibria, Prentice-Hall, Englewood Cliffs, New Jersey, 1967.
11. G. S. Canada and Faeth, G. M., "Fuel Droplet Burning Rates at High Pressures," Fourteenth Symposium (International) on Combustion, The Combustion Institute, Pittsburgh, Pennsylvania, pp. 1345-1354, 1973.
12. Harrje, D. T. (Ed.), Liquid Propellant Rocket Combustion Instability, NASA SP-194, National Aeronautics and Space Administration, Washington, D.C., pp. 128-138, 1972.
13. Faeth, G. M., "Monopropellant Droplet Burning at Low Reynolds Numbers," Combustion and Flame, Vol. 11, No. 2, pp. 167-174, 1967.
14. M. F. Heidmann and P. R. Wieber, "Analysis of Frequency Response Characteristics of Propellant Vaporization," AIAA Paper No. 66-604, 1966.
15. V. D. Agosta and S. S. Hammer, "Vaporization Response of Evaporating Drops with Finite Thermal Conductivity," NASA CR-2510, 1975.
16. Faeth, G. M., "Flame Zone Development of Monopropellant Droplets," Combustion and Flame, Vol. 12, No. 5, pp. 411-416, 1968.

17. Faeth, G. M., "Prediction of Pure Monopropellant Droplet Life Histories," AIAA J., Vol. 8, No. 7, pp. 1308-1314, July 1970.
18. Faeth, G. M., Karhan, B. L., and Yanyecic, G. A., "Ignition and Combustion of Monopropellant Droplets," AIAA J., Vol. 6, No. 4, pp. 684-689, April 1968.
19. Williams, F. A., Combustion Theory, first ed., Addison-Wesley, Reading, Massachusetts, pp. 231-245, 1965.
20. T'ien, J. S. and Sirignano, W. A., "Unsteady Thermal Response of the Condensed-Phase Fuel Adjacent to a Reacting Gaseous Boundary Layer," Thirteenth Symposium (International) on Combustion, The Combustion Institute, Pittsburgh, pp. 529-539, 1971.
21. Allison, C. B. and Faeth, G. M., "Decomposition and Hybrid Combustion of Hydrazine, MMH and UDMH as Droplets in a Combustion Gas Environment," Combustion and Flame, Vol. 19, No. 2, pp. 213-226, 1972.
22. Zeldovich, Ya. B., "On the Combustion Theory of Powder and of the Explosives," Zhurnal Eksperimental'noi i Teoreticheskoi Fiziki, Vol. 12, No. 11-12, p. 498, 1942.
23. Turk, S. L., et al, "Dynamic Responses of Solid Rockets during Rapid Pressure Change," J. Spacecraft and Rockets, Vol. 10, No. 2, pp. 137-142, 1973.
24. Summerfield, M., et al, "Theory of Dynamic Extinguishment of Solid Propellants with Special Reference to Nonsteady Heat Feedback Law," J. Spacecraft and Rockets, Vol. 8, No. 3, pp. 251-258, 1971.
25. Krier, H., et al, "Nonsteady Burning Phenomena of Solid Propellants: Theory and Experiments," AIAA J., Vol. 6, No. 2, pp. 178-185, 1968.

REPORT DISTRIBUTION LIST

NASA-Lewis Research Center Attn: Dr. R. J. Priem/MS 500-204 21000 Brookpark Road Cleveland, OH 44135 (2 copies)	Aerojet Liquid Rocket Company Attn: David A. Fairchild Bldg. 20001/Sec. 9732 P. O. Box 13222 Sacramento, CA 95813
NASA-Lewis Research Center Attn: N. T. Musial/MS 500-311 21000 Brookpark Road Cleveland, OH 44135	Aerojet General Corporation Propulsion Division Attn: R. Stiff P. O. Box 15847 Sacramento, CA 95803
NASA-Lewis Research Center Attn: Library/MS 60-3 21000 Brookpark Road Cleveland, OH 44135	Aerospace Corporation Attn: O. W. Dykema P. O. Box 92957 Los Angeles, CA 90045
NASA-Lewis Research Center Attn: Report Control Office/MS 5-5 21000 Brookpark Road Cleveland, OH 44135	Aerospace Corporation Attn: Library-Documents 2400 E. El Segundo Boulevard Los Angeles, CA 90045
NASA-Lewis Research Center Attn: E. A. Bourke/MS 500-205 21000 Brookpark Road Cleveland, OH 44135	Air Force Rocket Propulsion Lab. (RPM) Attn: Library Edwards, CA 93523
NASA Headquarters Attn: RPS/Robert A. Wasel 600 Independence Ave., SW, Rm 526 Washington, DC 20546	Air Force Office of Scientific Research Chief Propulsion Division Attn: Dr. J. F. Masi (NAE) 1400 Wilson Boulevard Arlington, VA 22209
NASA-Lewis Research Center Attn: Procurement Section Mail Stop 500-313 21000 Brookpark Road Cleveland, OH 44135	Air Force Rocket Propulsion Laboratory Attn: Daweel George Edwards, CA 93523
NASA-Lyndon B. Johnson Space Center Attn: EP/Joseph G. Thibodaux Houston, TX 77058	AFAPL Research & Technology Div. AF Systems Command U.S. Air Force Attn: Library/APRP Wright Patterson AFB, OH 45433
NASA-George C. Marshall Space Flight Center Attn: S&E-ASTN-PP/R. J. Richmond Huntsville, AL 35812	Air Force Rocket Propulsion Laboratory Attn: Richard R. Weiss Edwards, CA 93523
NASA Scientific & Technical Information Facility - Acquisitions Branch P.O. Box 8757 Baltimore/Washington International Airport Baltimore, MD 21240 (10 copies)	AFAPL Attn: Frank D. Stull (RJT) Wright Patterson AFB, OH 45433

Army Ballistics Research Labs.
Attn: Austin W. Barrows
Code AMXBR-1B
Aberdeen Proving Grounds, MD 21005

Army Ballistic Research Labs.
Attn: Ingo W. May
Code AMXBR-1B
Aberdeen Proving Grounds, MD 21005

Army Material Command
Missile Systems Div.
Attn: Stephen R. Matos
Code AMCRD-MT
5001 Eisenhower Ave.
Alexandria, VA 22304

Air Force Systems Command
Arnold Engineering Development Center
Attn: Dr. H. K. Doetsch
Tullahoma, TN 37389

Aeronutronic Div. of Philco Ford Corp.
Technical Information Dept.
Ford Road
Newport Beach, CA 92663

Battelle Memorial Institute
Attn: Report Library, Room 6A
505 King Avenue
Columbus, OH 43201

Bell Aerosystems, Inc.
Attn: Library
Box 1
Buffalo, NY 14205

Bell Aerospace Company
Attn: T. F. Ferger
Post Office Box 1
Mail Zone, J-81
Buffalo, NY 14205

Bureau of Naval Weapons
Department of the Navy
Attn: Library
Washington, DC

Brooklyn Polytechnic Institute
Long Island Graduate Center
Attn: V. D. Agosta
Route 110
Farmingdale, NY 11735

California Institute of Technology
Jet Propulsion Laboratory
Attn: Fred E. C. Culick
4800 Oak Grove Drive
Pasadena, CA 91103

California Institute of Technology
Jet Propulsion Laboratory
Attn: Jack H. Rupe
4800 Oak Grove Drive
Pasadena, CA 91103

California State University Sacramento
School of Engineering
Attn: Frederick H. Reardon
6000 J. Street
Sacramento, CA 95819

Chemical Propulsion Information Agency
Johns Hopkins University/APL
Attn: T. W. Christian
8621 Georgia Avenue
Silver Spring, MD 20910

Colorado State University
Attn: Charles E. Mitchell
Fort Collins, CO 80521

Frankford Arsenal
Attn: Martin Visnov
NDP-R, Bldg. 64-2
Bridge & Tacony Streets
Philadelphia, PA 19137

General Electric Company
Flight Propulsion Laboratory Dept.
Attn: D. Suichu
Cincinnati, OH 45215

Georgia Institute of Technology
Georgia Tech. Res. Inst.
Attn: Warren C. Strahle
Atlanta, GA 30332

Georgia Institute of Technology
Georgia Tech. Res. Inst.
Attn: Ben T. Zinn
Atlanta, GA 30322

Melvin Gerstein
P. O. Box 452
Altadena, CA 91001

Marquardt Corporation
16555 Saticory Street
Box 2013 - South Annex
Van Nuys, CA 91409

Massachusetts Institute of Technology
Department of Mechanical Engineering
Attn: T. Y. Toong
77 Massachusetts Avenue
Cambridge, MA 02139

McDonald Douglas Corporation
McDonnell Douglas Astronautics Co.
Attn: William T. Webber
5301 Bolsa Ave.
Huntington Beach, CA 92647

D. E. Mock
Advanced Research Projects Agency
Washington, DC 20525

Lockheed Aircraft Corporation
Lockheed Propulsion Co., Div.
Attn: Norman S. Cohen
P. O. Box 111
Redlands, CA 92373

Naval Postgraduate School
Department of Aeronautics
Attn: David W. Netzer
Monterey, CA 93940

Naval Underwater Systems Center
Energy Conversion Dept.
Attn: Robert S. Lazar, Code 5B331
Newport, RI 02840

Naval Weapons Center
Attn: Edward W. Price, Code 608
China Lake, CA 93555

Naval Weapons Center
Attn: Charles J. Thelen, Code 4505
China Lake, CA 93555

Naval Postgraduate School
Department of Aeronautics
Attn: Allen F. Fuhs
Monterey, CA 93940

Ohio State University
Department of Aeronautical and
Astronautical Engineering
Attn: R. Edse
Columbus, OH 43210

Pennsylvania State University
Mechanical Engineering Department
Attn: G. M. Faeth
207 Mechanical Engineering Bldg.
University Park, PA 16802

Princeton University
Forrestal Campus Library
Attn: Irvin Glassman
P. O. Box 710
Princeton, NJ 08450

Princeton University
Forrestal Campus Library
Attn: David T. Harrje
P. O. Box 710
Princeton, NJ 08540

Princeton University
Forrestal Campus Library
Attn: Martin Summerfield
P. O. Box 710
Princeton, NJ 08540

Propulsion Sciences, Inc.
Attn: Vito Agosta
P. O. Box 814
Melville, NY 11746

Purdue University
Jet Propulsion Laboratory
Project Squid
Attn: Robert Goulard
West Lafayette, IN 47907

Purdue University Res. Foundation
School of Mechanical Engineering
Attn: John R. Osborn
Thermal Sci. Propulsion Center
West Lafayette, IN 47906

Purdue University Res. Foundation
School of Mechanical Engineering
Attn: Bruce A. Reese
Thermal Sci. Propulsion Center
West Lafayette, IN 47906

Research and Development Associates
 Attn: Raymond B. Edelman
 P.O. Box 3580
 525 Wilshire Blvd.
 Santa Monica, CA 90402

Rockwell International Corporation
 Rocketdyne Division
 Attn: L. P. Combs, D/991-350
 Zone 11
 6633 Canoga Avenue
 Canoga Park, CA 91304

Rockwell International Corporation
 Rocketdyne Division
 Attn: James A. Nestlerode
 Dept. 596-124, AC46
 6633 Canoga Avenue
 Canoga Park, CA 91304

Rockwell International Corporation
 Rocketdyne Division
 Attn: Carl L. Oberg
 Dept. 589-SS11
 6633 Canoga Avenue
 Canoga Park, CA 91304

Rockwell International Corporation
 Rocketdyne Division
 Attn: Library Dept. 596-306
 6633 Canoga Avenue
 Canoga Park, CA 91304

Stanford Research Institute
 333 Ravenswood Avenue
 Menlo Park, CA 94025

Susquehanna Corporation
 Atlantic Research Division
 Attn: Library
 Shirley Highway and Edsall Road
 Alexandria, VA 22314

TISIA
 Defense Documentation Center
 Cameron Station, Bldg. 5
 5010 Duke Street
 Alexandria, VA 22314

D. E. Cooker
 Army Ballistics Research Lab.
 AMXBR-1B
 Aberdeen Proving Grounds,
 Maryland 21005

Tennessee Technological University
 Dept. of Mech. Engr.
 Attn: Kenneth R. Purdy
 P.O. Box 5014
 Cookeville, TN 38501

Textron, Inc.
 Bell Aerospace, Div.
 Research Department
 Attn: John H. Morgenthaler, C-84
 P.O. Box One
 Buffalo, NY 14240

TRW, Inc.
 TRW Systems Gp.
 Attn: A. C. Ellings
 One Space Park
 Redondo Beach, CA 90278

TRW Systems
 Attn: G. W. Elverun
 One Space Park
 Redondo Beach, CA 90278

TRW Systems Group
 STL Tech. Lib. Doc. Acquisitions
 One Space Park
 Redondo Beach, CA 90278

Tulane University
 Attn: J. C. O'Hara
 6823 St. Charles Ave.
 New Orleans, LA 70118

Ultrasystems, Inc.
 Attn: Thomas J. Tyson
 500 Newport Center Dr.
 Newport Beach, CA 92660

United Aircraft Corporation
 Pratt & Whitney Aircraft Division
 Attn: Thomas C. Mayes
 P.O. Box 2691
 West Palm Beach, FL 33402

United Aircraft Corporation
 Pratt & Whitney Division
 Florida Research & Development Center
 Attn: Library
 West Palm Beach, FL 33402

United Aircraft Corporation
Attn: R. H. Woodward Waesche
400 Main Street
East Hartford, CT 06108

United Aircraft Corporation
United Technology Center
Attn: Library
P. O. Box 358
Sunnyvale, CA 94088

University of California
Aerospace Engineering Dept.
Attn: F. A. Williams
Post Office Box 109
LaJolla, CA 92037

University of California, Berkeley
Dept. of Mechanical Engineering
Attn: A. K. Oppenheim
Berkeley, CA 94720

University of Illinois
Aeronautics/Astronautic Engr. Dept.
Attn: R. A. Strehlow
Transportation Bldg., Room 101
Urbana, IL 61801

University of Michigan
Attn: James A. Nicholls
P. O. Box 622
Ann Arbor, MI 48107

University of Utah
Dept. of Chemical Engineering
Attn: Alva D. Baer
Park Bldg., Room 307
Salt Lake City, UT 84112

University of Wisconsin
Mechanical Engineering Dept.
Attn: P. S. Myers
1513 University Avenue
Madison, WI 53706

United States Naval Research Laboratory
Director (Code 6180)
Attn: Library
Washington, DC 20390

Virginia Polytechnic Institute State
University
Attn: J. A. Schetz
Blacksburg, VA 24061

Office of Assistant Director
(Chemical Technician)
Office of the Director of Defense
Research & Engineering
Washington, DC 20301